Journal of Marine Research, 66, 645–663, 2008

Combined effect of wind-forcing and isobath divergence on upwelling at Cape Bathurst, Beaufort Sea

by William J. Williams[1,2] and Eddy C. Carmack[1]

ABSTRACT

Cape Bathurst is at the northeastern end of the Canadian Beaufort Shelf in the southeastern Beaufort Sea where the continental shelf abruptly ends at Amundsen Gulf. In this area, the steep slope east of the cape joins the relatively flat shelf immediately north of the cape leading to strong isobath divergence at the cape. Hydrographic and satellite data show upwelling of nutrient-rich, Pacific-origin water to the surface at Cape Bathurst when surface stress is upwelling-favorable for the Canadian Beaufort Shelf. We suggest that this enhanced upwelling is forced by the adjustment of the along-shelf flow (that is part of upwelling circulation) to the isobath divergence at the cape. Mooring and drifter data near Cape Bathurst also support this, showing swift, surface-intensified along-isobath flow during upwelling-favorable surface stress. Benthic samples near the cape show high numbers and diversity of organisms which suggest that nutrients brought to the surface by upwelling allow additional primary production in the region that ultimately feeds the benthos.

1. Introduction

The Canadian Beaufort Shelf in the southeastern Beaufort Sea is a relatively flat, wide and shallow shelf (width = 115 km; shelf-break depth = 60–80 m) that stretches between two fjord-like features: Mackenzie Trough in the southwest and Amundsen Gulf in the northeast (Fig. 1(a)). Cape Bathurst lies at the northeastern end on the boundary between Amundsen Gulf and the Canadian Beaufort Shelf. On the eastern side of Cape Bathurst the sea floor slopes steeply down into Amundsen Gulf so that the distance between the 0 and 60 m isobaths is only 8 km (Fig. 1(b)). The resulting strong divergence of isobaths near Cape Bathurst as the 0–60 m topography widens from 8 km on the eastern side of the cape to 115 km on the Canadian Beaufort Shelf (a widening of ~15 times) sets the regional conditions for topographically-enhanced shelf-break upwelling.

Examples in the literature of topographically-induced upwelling include: Swift and Aagaard (1976), which examined upwelling in Samalga Pass in the Aleutian Island Chain and concluded that it was driven by subsurface convergence of flow following the topography; Janowitz and Pietrafesa (1982), which considered the inviscid vorticity dynamics of a boundary current over variable shelf topography and applied it to the Gulf

1. Institute of Ocean Sciences, 9860 West Saanich Road, Sidney, British Columbia, V8L 4B2, Canada.
2. Corresponding author. ***email: Bill.Williams@pac.dfo-mpo.gc.ca***

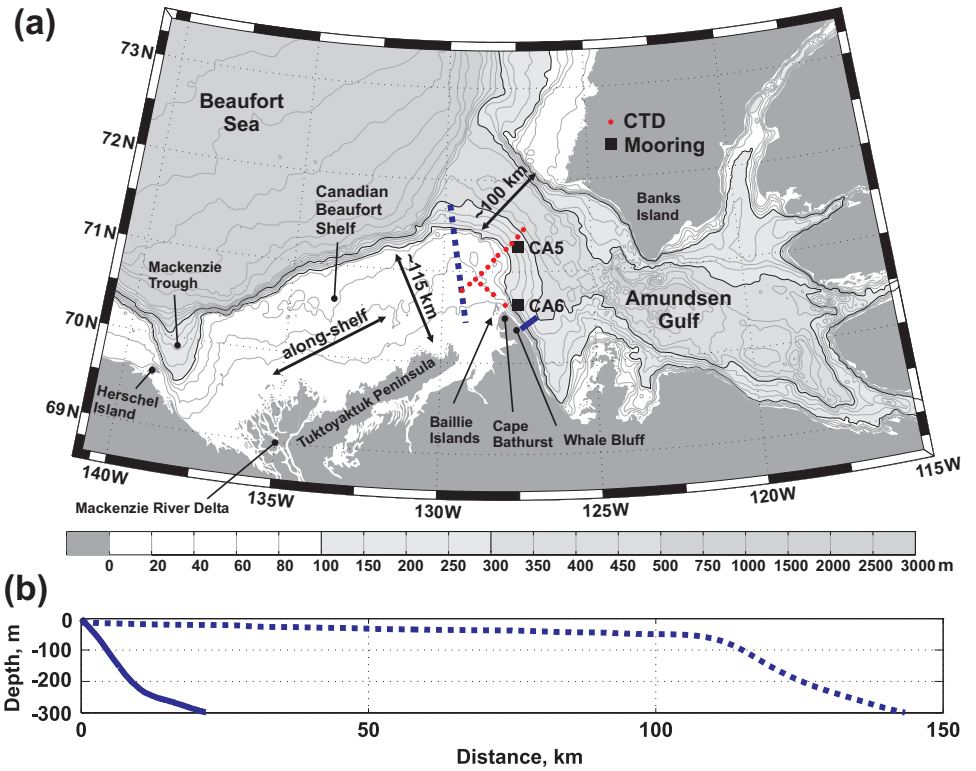

Figure 1. (a) A map of the southeastern Beaufort Sea showing the Canadian Beaufort Shelf and Amundsen Gulf. The red circles show the location of the CTD casts for the two hydrographic sections and the black squares show the locations of moorings CA5 and CA6. The along-shelf direction used is also marked where up-shelf is toward Mackenzie Trough and down-shelf toward Cape Bathurst. (b) Two depth profiles, one from the eastern side of Cape Bathurst from Whale Bluff into Amundsen Gulf (blue) and the other from the western side of Cape Bathurst across the Canadian Beaufort Shelf (blue dotted). The location of the profiles is shown on the map.

Stream over the northeastern Florida shelf; Oke and Middleton (2000), which used a numerical model of the continental shelf off eastern Australia to show that convergence of isobaths there causes acceleration of the East Australia Current that prevents the geostrophic shut down of the bottom boundary layer and thus allows persistent upwelling; and finally Pringle (2002), which considered the adjustment of wind-forced barotropic upwelling and downwelling circulation (with linear bottom friction) to a change in shelf width with application to the California Shelf.

In the following we present satellite images, wind estimates, hydrographic, drifter and mooring data to show enhanced wind-driven upwelling near Cape Bathurst associated with the strong isobath divergence. We conclude by considering the importance of upwelling at Cape Bathurst to the regional ecosystem and predict other sites where this type of upwelling may occur.

An along-shelf and cross-shelf frame of reference is used for wind and currents over the Canadian Beaufort Shelf. Along-shelf in the direction of Kelvin wave propagation (cyclonic, toward Amundsen Gulf) is called *down-shelf* and is taken as 052°T. Along-shelf in the direction of the mean circulation of the Beaufort Gyre (anticyclonic, toward the Alaskan Beaufort Shelf) is called *up-shelf* and taken as 232°T. Note that wind- or ice-stress in the up-shelf direction is the direction that is upwelling favorable.

2. Wind stress

Wind data were obtained from the National Centers for Environmental Prediction (NCEP) 6 hourly, 10 m wind fields. Wind stress for the Canadian Beaufort Shelf was estimated by assuming ice-free conditions and using the bulk formula $\boldsymbol{\tau}_{\mathbf{wind}} = \rho_a C D_{\text{air-water}} |\mathbf{U}|\mathbf{U}$ where ρ_a (1.2 kg/m^3) is the density of air, $CD_{\text{air-water}}$ (0.0015) is the 10-m drag coefficient (Fairall *et al.,* 1996) and **U** is the wind velocity (m/s). The average wind stress for the 10 NCEP grid points that surround the Canadian Beaufort Shelf is reported here. When sea ice is present, ice motion is forced by the wind, water velocity and internal ice stress while calculation of ice-ocean surface stress depends on the relative velocity between the ice and water and the roughness of the underside of the ice. Because we do not know ice roughness well, we do not attempt to calculate surface stress on the ocean due to the ice motion. Instead we use $|\mathbf{U_{ICE}}|\mathbf{U_{ICE}}$ from the ADCP records of two moorings near the center of the Canadian Beaufort Shelf as a general indication of the magnitude and direction of the ice-ocean stress (Williams *et al.,* 2008). The two moorings were Site 1 at 70°20′N, 133°44.4′W in 57 m of water and Site 2 at 70°59.3′N, 133°45.0′W in 116 m of water.

3. Spatial pattern of upwelling from surface temperature images

a. Summer

During spring and summer, surface waters over the Canadian Beaufort Shelf typically warm from near-freezing-point winter temperatures up to a maximum of ~12°C (Carmack and Macdonald, 2002). This warming is due both to seasonal solar heating and to the influx of warm Mackenzie River water which forms a large, irregular and surface-trapped plume (Yankovsky and Chapman, 1997) over the Canadian Beaufort Shelf (Carmack and Macdonald, 2002). The maximum sea-surface temperature is that of Mackenzie River water exiting the Mackenzie River delta, but the temperature of the plume remains high due to its low salinity, which reduces mixing with the underlying cold, relatively-salty water, and is enhanced by its high turbidity (providing a high light extinction coefficient) and its shallowness (it is only about 8-m thick and solar heating will mostly be contained in this layer).

Unequivocal evidence of upwelling is shown by sea-surface temperature (SST) images of Cape Bathurst and the Canadian Beaufort Shelf (Fig. 2). These images were taken in summer and fall during relatively ice-free conditions and during periods when the local

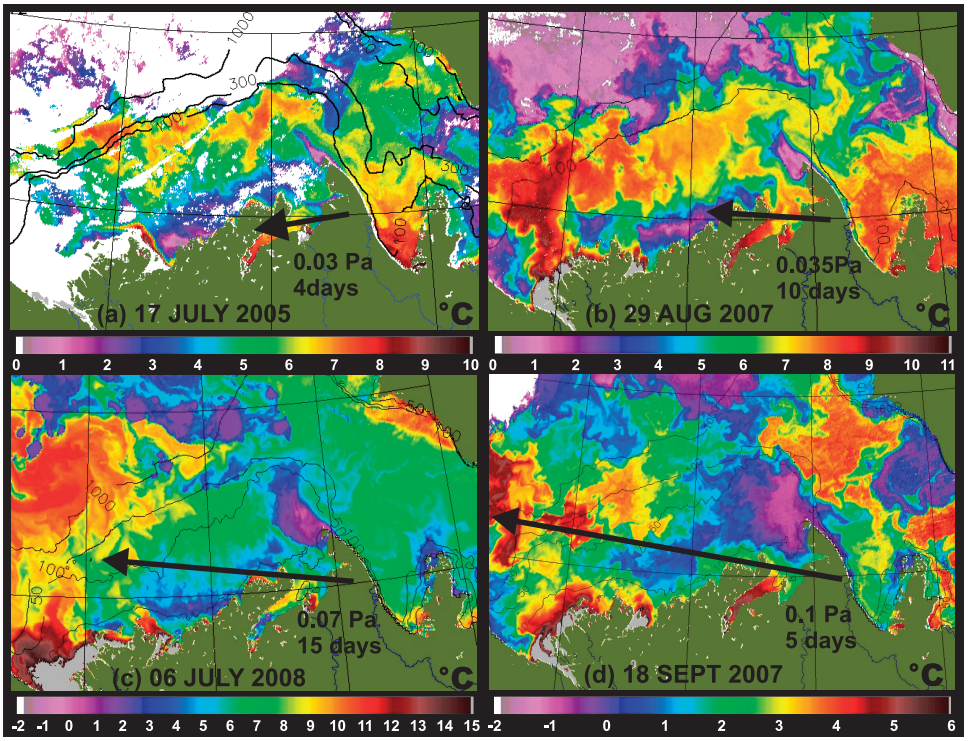

Figure 2. Sea-surface temperature images (prepared by Mike Schmidt) of the Canadian Beaufort Shelf and Amundsen Gulf showing upwelling of cold water at Cape Bathurst. The arrows are the mean NCEP wind stress for the period of upwelling-favorable winds prior to the image.

NCEP-derived wind stress was upwelling-favorable for the Canadian Beaufort Shelf. Cold areas in these images are either where the warm surface water has been pushed away by the cold underlying water upwelling to the surface (at Cape Bathurst and along the Tukoyaktuk Peninsula) or areas that are under the influence of sea ice and ice melt (in the north and along the coast of Banks Island).

In each satellite image, the warmer surface waters associated with the Mackenzie plume have been advected offshore along the Tuktoyaktuk Peninsula thus exposing the cold water underneath. This appears to be due to wind-driven Ekman transport from the upwelling-favorable wind stress. The plume responds strongly to the wind since all the Ekman transport is essentially confined to within the thin surface layer of plume water (~8 m thick) by the strong stratification at its base (Fong and Geyer, 2001). Near the Mackenzie River delta the warm plume water tends to remain connected to the shore, despite the offshore Ekman transport, which is expected from the numerical experiments of Fong and Geyer (2001).

At Cape Bathurst there is a distinctive patch of very cold water in each image that

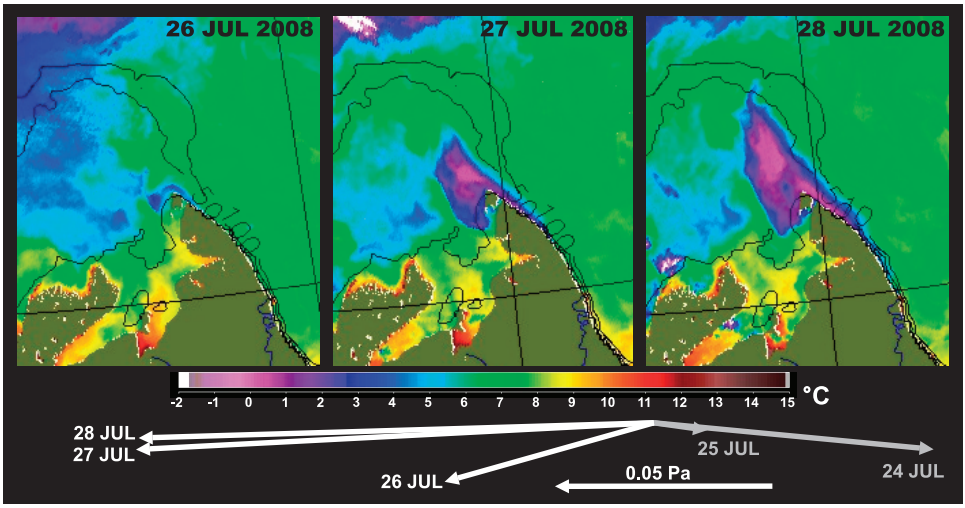

Figure 3. A sequence of sea-surface temperature images of Cape Bathurst taken starting at the onset of upwelling-favorable wind stress. The evolution of the daily averaged wind stress is shown below, beginning two days before the first satellite image.

extends from Whale Bluff on the eastern side of the cape 60–80 km northwest over the Canadian Beaufort Shelf. The average NCEP-derived wind stress for the duration of the upwelling-favorable conditions is also shown for each image in Figure 2. The cold patch varies in size and shape, but appears to be larger under larger wind stress: the patch is smallest in (a) and largest in (d). The growth of the patch of cold water at the cape was observed for an upwelling-favorable wind stress event in July 2008 (see Fig. 3). The images show the patch growing rapidly during the first three days of upwelling-favorable wind stress, which matches the barotropic spin-down time scale for the shelf circulation (one to three days) discussed in Section 5. After three days of upwelling wind stress there were no further satellite images available due to cloud cover.

Cloud-free satellite images of the Canadian Beaufort Shelf and Amundsen Gulf are rare so that it has not been possible to calculate unambiguous correlations between wind stress direction and the strength and extent of the patch of cold, upwelled water at Cape Bathurst. The cloud-free images are also biased toward wind forcing from the east (upwelling-favorable) as these are often associated with anti-cyclonic atmospheric circulation which tends to bring clear skies (Humfrey Melling, pers. comm.). However, since July 2004 the relatively cloud- and ice-free SST images of the Canadian Beaufort Shelf have been compiled by Mike Schmidt. In this image set, coastal upwelling along the Tuktoyaktuk Peninsula and upwelling at Cape Bathurst always occur together, suggesting that it is the broad upwelling circulation over the entire Canadian Beaufort Shelf that leads to localized shelf-break upwelling at the cape.

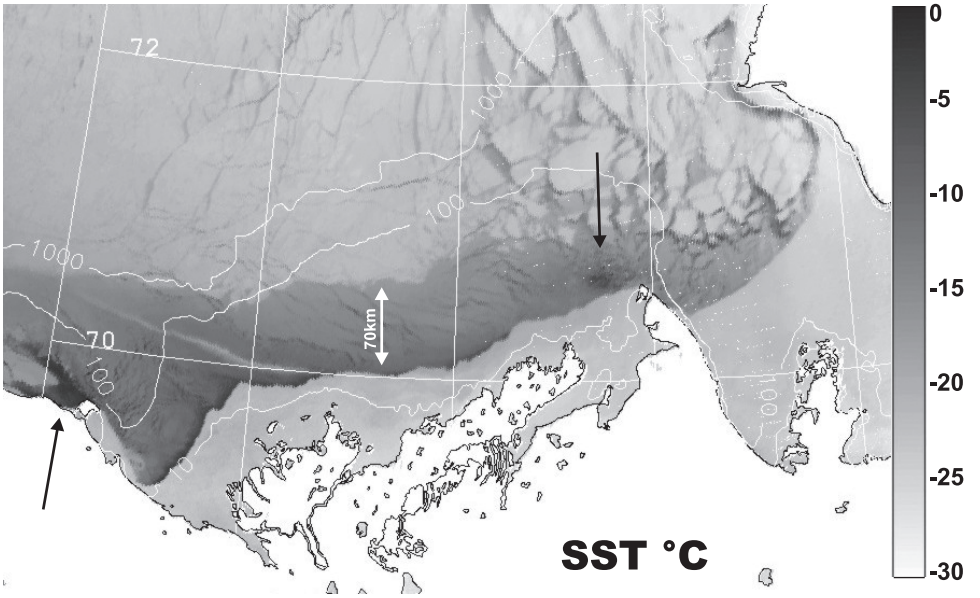

Figure 4. A surface temperature image of the Canadian Beaufort Shelf at 21:35 UTC on 4 March 2003 (prepared by Mike Schmidt) showing a flaw lead that developed from westward wind and ice motion and polynyas at Cape Bathurst and Herschel Island. This 1 km resolution image was prepared by Mike Schmidt and is from the Aqua satellite. The 10, 100 and 1000-m depth contours are marked; the 100-m contour approximately delineates the shelf-break.

b. Winter

In winter there can be periods of upwelling-favorable surface stress caused by wind-forced ice motion (Williams *et al.,* 2008). Such forcing also acts to move the mobile pack ice away from the stationary landfast ice, thus forming so-called flaw leads. Figure 4 is a surface temperature image of the Canadian Beaufort Shelf at 21:35 UTC on 4 March 2003. It clearly shows a flaw lead (the region of recently refrozen grey ice between the landfast ice and the mobile pack ice) that developed from westward wind and ice motion (Williams *et al.,* 2008). The upwelling-favorable wind stress began on 26 February and the flaw lead was close to its maximum width on 4 March. Grey ice fills the 70 km-wide flaw lead except at the landfast edge of the lead where there is a thin strip of open water that shows as relatively warm (dark) in the image. This open water exists because ice that forms there is pushed away from the landfast ice edge by the wind (Williams *et al.,* 2007; Pease, 1987). Arrows on the figure show two locations (one at Cape Bathurst and one west of Herschel Island) where there are larger areas of open water (polynyas). At Cape Bathurst we expect the polynya is due to the upwelling there, which we associate with isobath divergence in this paper. West of Herschel Island it is possible that both the known upwelling in Mackenzie Trough (Carmack and Kulikov, 1998; Williams *et al.,* 2006) and the isobath

divergence on the northeastern side of Herschel Island contribute to the shelf-break upwelling, while the island itself blocks ice advected from the east.

There are two contributory factors for the polynyas in these locations: (1) surface flow advects the frazil ice away from the landfast ice edge and from Herschel Island, or (2) the upwelling flow brings heat to the surface so that ice does not form. If the polynyas were formed solely by advection of frazil ice, we would expect to see some effect of this where the upwelling flows are fastest at the constrictions in bathymetry on the eastern side of Cape Bathurst and on the northeastern side of Herschel Island. The polynyas do not extend into these areas, however, so we consider the possibility of the upwelled water bringing heat to the surface. A crude estimate of the heat flux brought to the surface by upwelling can be made by assuming that all the along-shelf flow in the upwelling circulation over the shelf is supplied by upwelling at the cape from 80–100 m deep near the temperature minimum of the Pacific water and that all of this upwelling reaches the surface and releases its excess heat to the atmosphere. The presumption that all of the upwelling reaches the surface is an upper limit to the heat flux. The assumption of upwelling from 80–100 m deep is based on temperature-salinity data (see Section 3) and is conservative in terms of heat flux since it is near the temperature minimum of the Pacific water. To estimate the volume flux we use a 20 cm s^{-1} along-shelf flow over the 70 km-wide outer portion of the shelf between the edge of the landfast ice ($\sim$20 m isobath) and the shelfbreak ($\sim$60 m isobath). The Pacific water is about 0.3°C above its freezing point (see Fig. 7) which, combined with the volume flux, yields a possible heat flux to the surface of $\sim 7 \times 10^{11}$ W. We estimate the heat flux to the atmosphere over open water to be $\sim$700 W m^{-2}. This estimate is comprised of an upward sensible heat flux of about 400 W m^{-2} (calculated using a wind speed of $\sim$10 m s^{-1} and an air-water temperature difference of 25°C) and an upward long-wave radiative heat loss of about 300 W m^{-2} over open water. We assume that downward long-wave radiation is negligible, since the satellite image is cloud free, and that incident short-wave radiation is also negligible at this latitude and time of year. Equating the potential upwelling heat flux with the atmospheric heat flux gives a possible 1000 km^2 or equivalently a 35 km diameter circle, ice free due to upwelling at Cape Bathurst. This is somewhat larger than the polynya shown in Figure 4 at Cape Bathurst but is of the correct order of magnitude. The polynya west of Hershel Island is bigger than that at Cape Bathurst and this is possibly due to the combination of Mackenzie Trough and Herschel Island producing a larger amplitude upwelling there that brings warmer water to the surface (Williams *et al.,* 2006).

We conclude that the polynyas at Herschel Island and Cape Bathurst in Figure 4 are possibly due to heat flux to the surface. It is worth reiterating that the upwelling circulation that brings the heat to the surface is driven by surface stress due to the wind and ice motion so that these polynyas are essentially wind forced, as is the flaw lead. When the wind and ice motion cease, the upwelling circulation decays and the additional heat flux to the surface (required to maintain open water) stops.

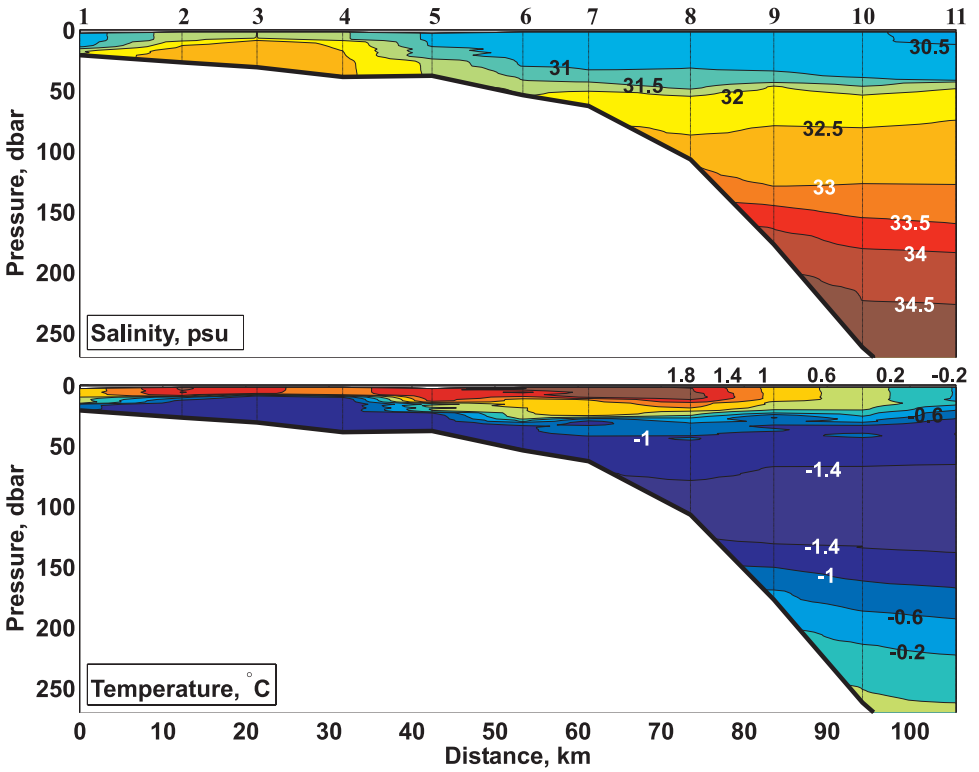

Figure 5. A hydrographic section taken on 17 June 2004 from the Canadian Beaufort Shelf into Amundsen Gulf (see Fig.1 for location) showing (a) salinity and (b) temperature. Each CTD cast is numbered for reference with Figure 7 and marked with a vertical dotted line.

4. Hydrographic sections

While the cold surface water at Cape Bathurst in the satellite images shows that upwelling is occurring there, it does not show the depth of upwelling. For this we need hydrographic sections, and particularly salinity since salinity largely determines density in the Arctic Ocean and monotonically increases with depth.

Two hydrographic sections that crossed the location of upwelled water at Cape Bathurst as seen in sea-surface temperature images were done in mid June 2004 using a Seabird 9/11 CTD (see Fig. 1 for locations of the section data). The Amundsen Gulf section (Fig. 5) was sampled on the 17th June 2004 at the end of a seven-day period of 0.037 Pa, upwelling-favorable (NCEP) wind stress for the Canadian Beaufort Shelf. The section shows a patch of high salinity water (32.5–33 psu) on the Canadian Beaufort Shelf between 12 and 32 km from the beginning of the section. The maximum salinity in the patch is 32.77 psu and, if upwelled from Amundsen Gulf, corresponds to a maximum upwelling depth of 110 m. In the section, the water at 110 m deep is not connected with the patch of high salinity water on the shelf suggesting that the upwelling occurred via an indirect route.

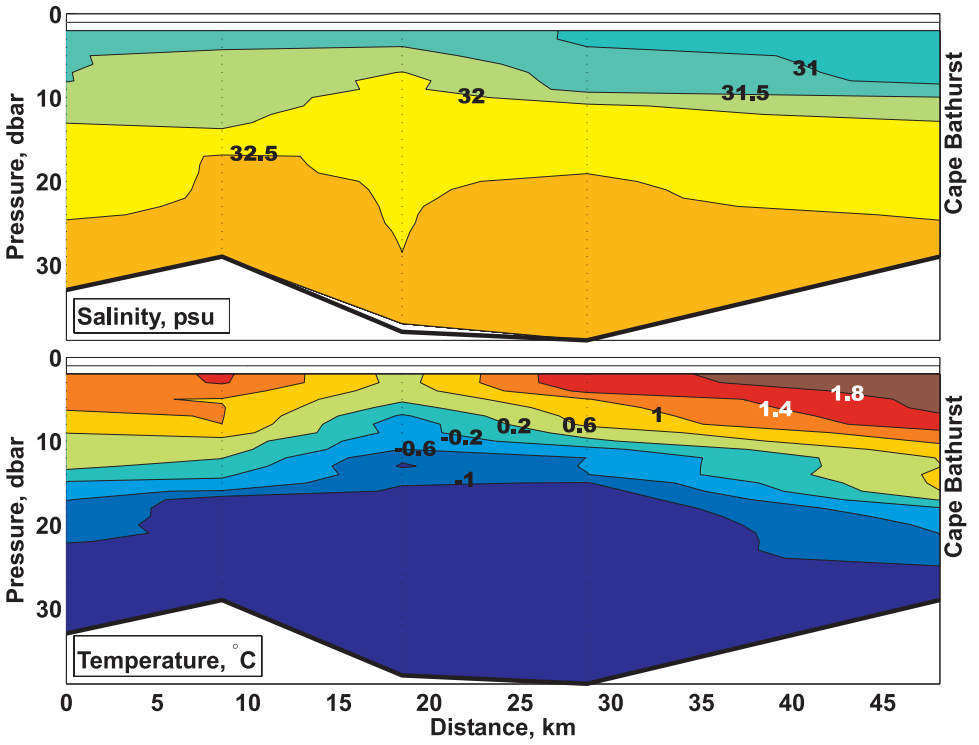

Figure 6. A hydrographic section taken on 21 June 2004 connecting the end of the section shown in Figure 5 to Cape Bathurst (see Fig. 1 for location). The sections shown are (a) salinity and (b) temperature with potential density (σ_θ) contours overlaid. Each CTD cast is marked with a vertical dotted line.

The hydrographic section that runs northwest of Cape Bathurst (Fig. 6) was sampled on the 21st June, 2004, four days after the Amundsen Gulf section and after a three-day period of 0.04 Pa, downwelling-favorable wind stress. Temperature and salinity are relatively uniform from one end of the section to the other and show the same high salinity upwelled water as the Amundsen Gulf section (see also Fig. 7 for the temperature-salinity plot of this data). We interpret the presence of upwelled water at the bottom of this section after three days of downwelling-favorable wind stress to be evidence of along-isobath transport of the water either from Cape Bathurst (if upwelling circulation has not spun down yet) or from the patch of upwelled water shown in the Amundsen Gulf section (during downwelling circulation). This interpretation follows the explanation for upwelling at Cape Bathurst given in Section 5, but either way this section demonstrates a connection of the salty, upwelled water to Cape Bathurst, as is found for the low-temperature patch of water in the sea-surface temperature satellite images.

The potential temperature-salinity plot of data from the two sections (Fig. 7) shows that water within the patch of upwelled water on the Canadian Beaufort Shelf (stations 2, 3 and

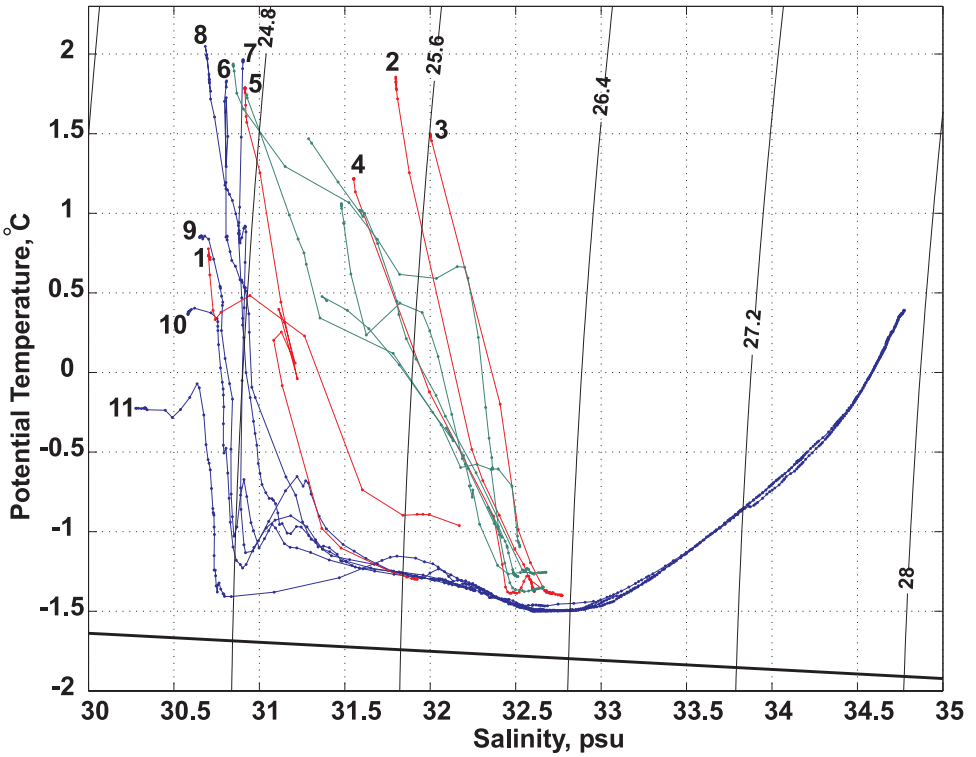

Figure 7. A temperature-salinity plot for the sections shown in Figures 5 and 6. Red is data from Figure 5 from the Canadian Beaufort Shelf, blue is data from Figure 5 from Amundsen Gulf and green is data from Figure 6. Each CTD cast from Figure 5 is numbered to correspond with that figure.

4 of Fig. 5) is warmer than water of the same salinity from Amundsen Gulf: the most saline upwelled water has warmed ~0.1°C from its origins near 110 m deep in Amundsen Gulf and the warmest upwelled water has warmed at least 2.5°C. This warming of high salinity near-surface water is a characteristic signature of summer upwelling. On the temperature-salinity plot (Fig. 7) the warm upwelled water does not lie on any reasonable mixing line between two other water masses and we infer from this that the warming must have occurred by the water upwelling to the surface and contact with the warmer atmosphere.

5. Mechanism of upwelling at a change in shelf width

Here we provide a simple summary of enhanced upwelling at a change in shelf width (isobath divergence) based on the linear, barotropic model of Pringle (2002) where an up-shelf wind stress is applied to a shelf that widens in the up-shelf direction. We do not consider Cape Bathurst as part of the circulation in Amundsen Gulf. This is a good place to begin, though we estimate later that, because of the extreme narrowing of the shelf past

Cape Bathurst, the flow there is nonlinear (the Rossby number is not small) and stratification is important (the flow has a scale similar to the baroclinic Rossby radius of deformation). Hence, a linear, barotropic model does not strictly apply.

Suppose a steady up-shelf wind stress is applied to a straight shelf of constant width. When using linear, barotropic dynamics the resulting steady upwelling circulation consists of offshore Ekman transport in the surface boundary layer, an equal onshore Ekman transport in the bottom boundary layer (the upwelling) and a geostrophically balanced up-shelf flow. The bottom boundary layer is caused by bottom friction associated with the up-shelf flow and during spin-up of the circulation, the up-shelf flow will accelerate until the onshore transport in the bottom boundary layer balances the offshore transport in the surface boundary layer. The spin-up time for this frictional balance to occur is estimated at one to three days using the frictional spin-down time H/r where H is the depth of the shelf-break and r is a linear bottom friction coefficient, typically $2\text{–}5 \times 10^{-4}$ m s^{-1} (Pringle, 2002). The frictional balance also gives the velocity of the along-shelf flow as $v_{Fr} = \tau/\rho r$ where τ is the wind stress and ρ is the water density. This velocity does not vary with depth, so it is easy to estimate the up-shelf transport as $T = A\tau/\rho r = HW\tau/2\rho r$ where A is the cross-sectional area of the water over the shelf, W is the shelf width, H is the depth at the shelf break and a linear depth profile is assumed. The up-shelf transport is linearly dependent on the shelf width so that there is more transport over a wide shelf than over a narrow shelf of the same shelf-break depth.

Now, if there is a change in shelf width such that the shelf widens up-shelf (see Fig. 8), the additional transport required over the wide shelf must cross the shelf-break in the vicinity of the change in shelf width. Pringle (2002) finds the additional cross-shelf flow to occur as upwelling in the bottom boundary layer at the change in width and down-shelf of it; an example of down-shelf propagation of information. The additional transport required is $T_A = T_W - T_N = H(W_W - W_N)\tau/2\rho r$ where T_W is the transport over the wide shelf, T_N is the transport over the narrow shelf, T_W is the width of the wide shelf and T_N is the width of the narrow shelf.

In this linear barotropic case, the mechanism of the additional upwelling is as follows. The geostrophic balance of the up-shelf flow constrains it to follow isobaths so that the up-shelf flow over the wide shelf must come from the region where the shelf is narrow. Since the isobaths are closer together on the narrow shelf, the up-shelf flow is faster there, which causes greater bottom friction and results in greater onshore transport (greater upwelling) in the bottom boundary layer. This additional upwelling supplies the additional up-shelf transport required over the wide up-shelf part. The maximum additional speed of the flow over the narrow shelf is $v_A = v_{Fr}(W_W/W_N - 1)$ and the additional Ekman transport in the bottom boundary layer (upwelling) is $E_A = rv_A/f = (W_W/W_N - 1)\tau/\rho f$. The minimum along-shelf distance L over which the up-shelf velocity must remain elevated in order to supply the up-shelf transport required by the wide shelf can be estimated by writing $T_A = E_A L$ which gives $L = W_N Hf/2r$. Larger values of L are expected as the additional up-shelf flow and bottom Ekman transport will decay away from

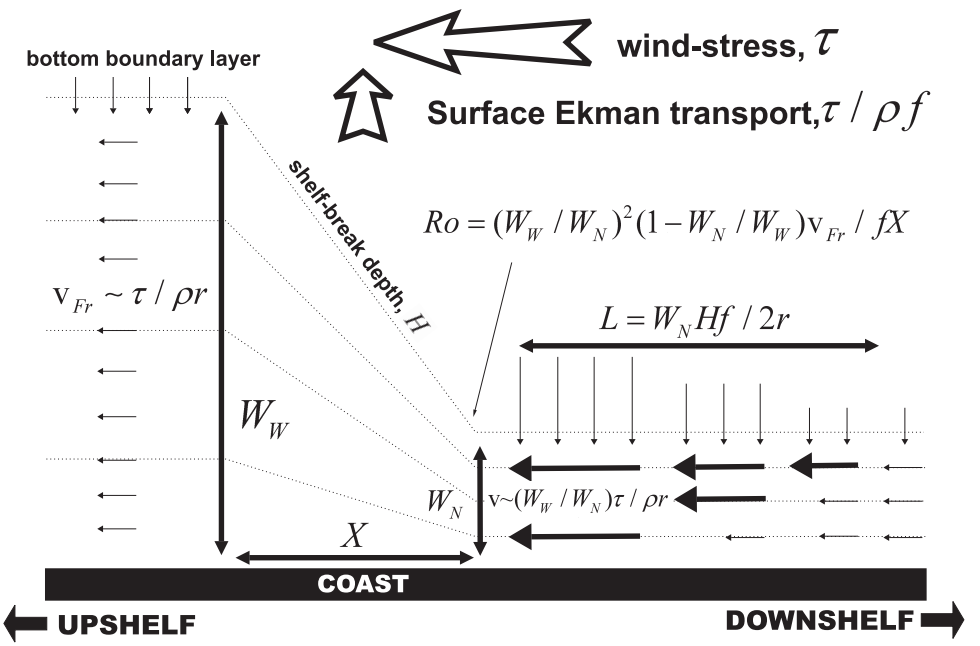

Figure 8. A cartoon of upwelling due to isobath divergence as described by Pringle (2002). We anticipate that a stratified, nonlinear version of this is occurring around Cape Bathurst.

the change in shelf width. The above argument can be ascribed to all isobaths over the shelf so the estimate L increases when moving offshore into deeper waters, and the effect of the change in shelf width persists longer in the downshelf direction near the shelf-break than it does near the coast.

Returning to the Canadian Beaufort Shelf, up-shelf flow over the Canadian Beaufort Shelf, if constrained to follow isobaths, must come from the region of narrow topography on the Amundsen Gulf side of Cape Bathurst (e.g. Whale Bluff) where the 0–60 m shelf topography is 15 times narrower than over the Canadian Beaufort Shelf. Applying the linear barotropic theory as a first estimate, and using $r = 5 \times 10^{-4}$ m s^{-1}, $\tau \sim 0.1$ Pa, $\rho =$ 1000 kg m^{-3}, $W_N \sim 8$ km and $W_W \sim 115$ km predicts that v ~ 3 m s^{-1} and $L \sim 25$ km (see Fig. 8). Satellite images of Figure 2 show the estimate for L to be somewhat reasonable: there is a thin strip of cold upwelled water against the coast which extends roughly 25 km south from Cape Bathurst along the Amundsen Gulf side of the cape in each image. We do not have water velocity measurements within the shelf-break depth off the coast near Cape Bathurst during upwelling events, but there is evidence from drifters: on 29 August 1987, during *downwelling-favorable* wind from the west, one drifter rounded the northern side of the Baillie Islands very close to shore at 3 m s^{-1} (Humfrey Melling pers. comm., Fig. 10). For the theory described here the direction of alongshelf flow simply reverses under downwelling-favorable wind stress as opposed to upwelling-favorable wind

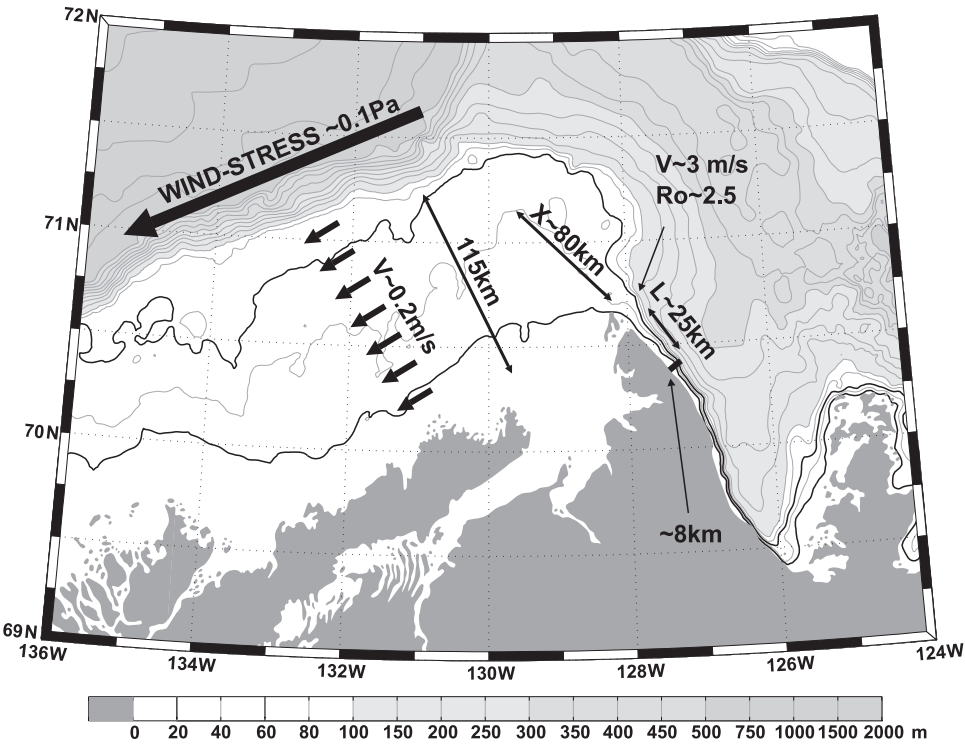

Figure 9. A map showing parameters and scales for the barotropic upwelling case at Cape Bathurst.

stress, so that these drifter data do provide evidence of the speed of wind-driven flows at Cape Bathurst.

A Rossby number for the flow at Cape Bathurst can be constructed by comparing along-shelf advection of along-shelf momentum with the cross-shelf Coriolis force assuming that the flow remains in cross-isobath geostrophic balance and follows isobaths. This gives the Rossby number $Ro = (W_W/W_N)^2(1 - W_N/W_W)v_{Fr}/fX$ where X is the length of the transition from the wide to the narrow shelf. At Cape Bathurst the ratio of the wide to narrow shelf is roughly 12 which occurs over a distance of about 80 km. Using an along-shelf velocity of 0.2 m s^{-1} over the wide shelf and taking $f = 1.37 \times 10^{-4}$ s^{-1} gives $Ro \sim 2.5$, suggesting that nonlinear advection is important at Cape Bathurst and that the flow may depart from geostrophic balance there.

In the region of upwelling on the eastern side of Cape Bathurst, baroclinic forces will be important as the Rossby radius of deformation is ~10 km which is similar to the width of the enhanced along-shelf flow that is expected over the 0–60 m topography. Also, during upwelling, isopycnals are tilted up toward the shore and, if the along-isobath flow remains in rough cross-shelf geostrophic balance, the thermal wind shear due to the tilted isopycnals will tend to reduce the flow velocity toward the bottom. A simple estimate of

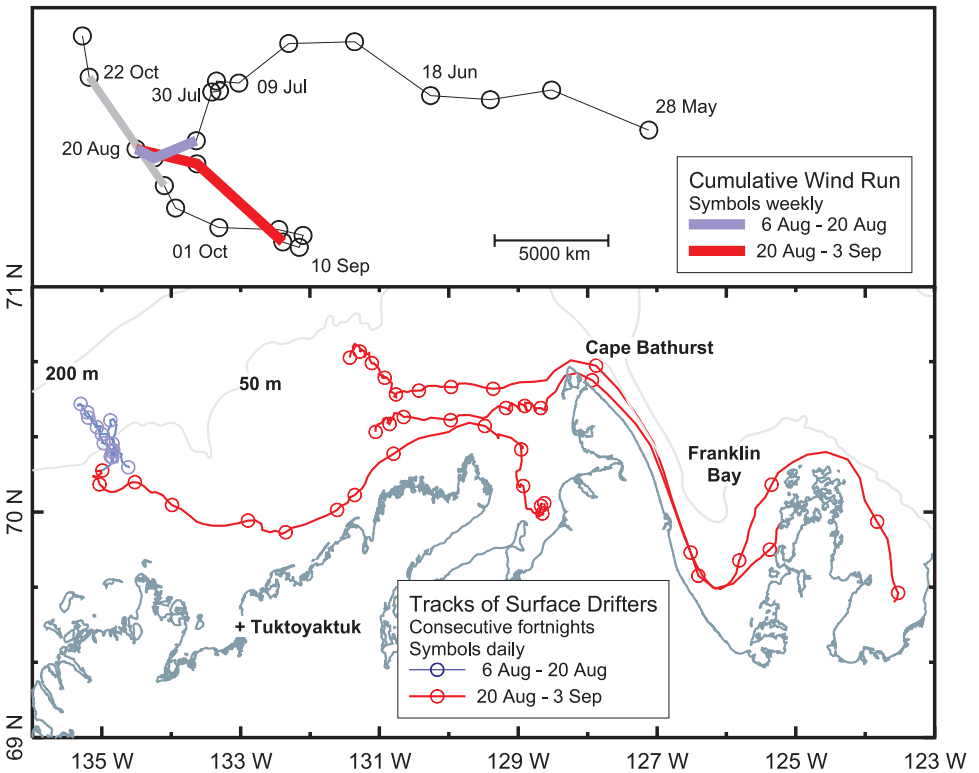

Figure 10. Surface drifter tracks around Cape Bathurst (bottom panel) and cumulative wind run (top panel) for August of 1987. The maximum speed of the drifters was close to 3 m s^{-1} near Whale Bluff. The cumulative wind run is a progressive vector of the wind velocity that encompasses the duration of the drifter deployment shown. The second week of the red-progressive vector (27 Aug–3 Sep) is ~5000 km long and so corresponds to a wind speed of around ~30 km/hr or 16 kts.

the size of this effect can be made by assuming that isopycnals upwell to become parallel to the bottom over the 0–60 m topography. This gives $\Delta v = gH\Delta\rho/fW_N\rho_0$ at the shelf-break depth H, where $\Delta\rho$ is the density difference between the surface and the bottom and ρ_0 is a reference density (1025 kg m^{-3}). On the eastern side of Cape Bathurst, $\Delta\rho \sim 3$ kg m^{-3} at $H = 60$ m which gives $\Delta v \sim 2$ m s^{-1}. This is of similar size to the estimate of 3 m s^{-1} for the barotropic flow and so baroclinic effects are likely of equal importance.

The reduction of along-shelf flow near the bottom due to baroclinic effects will reduce the bottom-stress and thereby reduce the upwelling volume flux in the bottom boundary layer. Smaller upwelling fluxes will require that the region of upwelling downshelf of Cape Bathurst is longer than the linear barotropic estimate (larger L) in order to give the same total upwelling flux. Moving downshelf from Cape Bathurst, the enhanced along-shelf flow will decay, and at some point the flow will become slow enough that isopycnals tilting

up toward shore bring the along-shelf bottom velocity to near zero. At this point the bottom-stress becomes small and the bottom boundary layer will shut down. This is the 'arrested' bottom boundary layer that has been well described in the literature (see Garrett *et al.* (1993) for a review). One important parameters controlling the arrest of the bottom boundary layer is the slope Burger number $S = \alpha N/f$ where α is the bottom slope and N is the buoyancy frequency (Chapman and Lentz, 2005). The slope Burger number is large on the eastern side of Cape Bathurst because of the steep slope and strong stratification ($S \sim 1$) and shut down of the bottom boundary layer is expected. In the satellite images shown, the upwelling front surfaces about 25 km south of Cape Bathurst and this may be the approximate location in which the bottom boundary layer shuts down.

In the above we consider the upwelling at Cape Bathurst to be due to the adjustment of the wind-forced, up-shelf flow to a change in shelf width around the cape. We do not consider the ~90° change in direction of the isobaths between the Canadian Beaufort Shelf and Amundsen Gulf because this change in direction mostly occurs over the shelf to the north and west of the cape. We also do not consider the mean circulation or wind-driven circulation of Amundsen Gulf partly because little is known about it. However, Amundsen Gulf can be considered a large undersea canyon that is four to five times wider than the baroclinic Rossby radius of deformation (based on the sill depth of Amundsen Gulf) and about half as wide as the barotropic Rossby radius (based on the shelf-break depth). As such, the baroclinic model results found in Hyun (2004) and the barotropic, geostrophic dynamics presented in Chen and Allen (1996) may give some indication of the wind-driven circulation of Amundsen Gulf and leave the possibility that the presence of Amundsen Gulf could contribute to the upwelling at Cape Bathurst.

6. Mooring data

Mooring data were collected in Amundsen Gulf ~20 km northeast of Cape Bathurst at CA6 (70°39.00′ N 127°32.85′ W, 205 m water depth) and ~85 km north-northeast of Cape Bathurst at CA5 (71°16.95′N 127°32.14′W, 201 m water depth) from September 2002 to September 2003 as part of the Canadian Arctic Shelf Exchange Study (see Fig. 1). The water velocity data shown here were from upward-looking ADCPs (RDI 300 kHz) located at approximately 95 m deep which recorded hourly data with 8 m bin sizes. The velocity time series shown here are low-pass filtered (half amplitude at 33-hour period), to remove variance dominated by tides and inertial waves, and then plotted at six hourly intervals.

Figure 11 shows velocity and salinity time series data for CA5 and CA6 with estimates of the along-shelf wind stress and ice stress for the Canadian Beaufort Shelf. In general, flow at CA5 and CA6 is predominantly in the local along-isobath direction and flow speeds during the period of winter ice cover (January–June) are less than those in the ice free period. However, the 10–80 m vertically averaged flow at CA6 is approximately 1.5 times faster than at CA5 (when averaged over the period of the mooring deployment) (see Table 1), suggesting that CA6 is close enough to Cape Bathurst to feel the amplification of the along isobath flow there. Also,

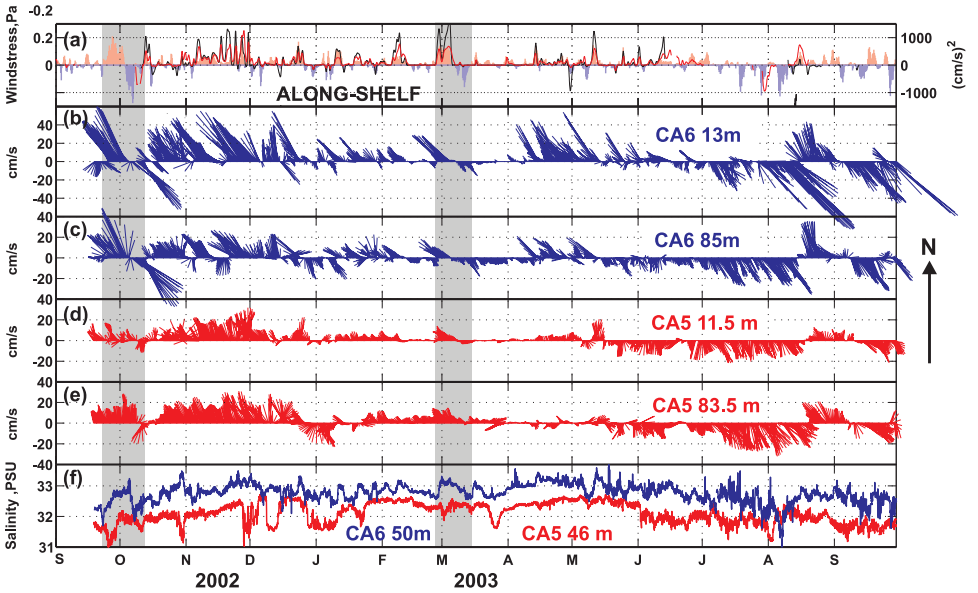

Figure 11. Time series data from moored instruments at sites CA5 and CA6 (see Fig. 1 for location). (a) Shows wind stress calculated from the 6 hourly NCEP re-analysis data set (red and blue sticks) and the square of the ice velocity as a proxy for 'ice-stress' at Site 1 (black) and Site 2 (red) calculated from ADCP data. Stick vectors of ADCP velocity for (b) CA6, 13-m deep, (c) CA6 85-m deep, (d) CA5 11.5-m deep and (e) CA5 83.5-m deep. North is toward the top of the page. (f) Salinity time series at CA6 50-m deep and CA5 46-m deep. A large, ice-free, upwelling event followed by a downwelling event occurred around the beginning of October 2002 and is highlighted by a grey band. The flaw lead event around the beginning of March 2003, which is shown in the satellite image in Figure 4, is also highlighted by a grey band.

the flow at CA6 is sheared so that it becomes faster towards the surface (see Table 1) and is consistent with thermal wind shear due to tilted isopycnals associated with upwelling or downwelling on the eastern side of the cape. In contrast, there is much less vertical shear at CA5 and the deeper flow is, on average, slightly faster than the near surface flow there (see Table 1).

Over the course of a year, there are numerous periods of upwelling and downwelling-

Table 1. Mean speeds calculated from the ADCP data from moorings CA5 and CA6. The means are calculated for the duration of the deployment (September 2002–September 2003). The 10–80 m mean speed is the vertical average over the range of the ADCP.

	ADCP depth bin	Mean speed	10–80 m mean speed
CAS	11.5 m (top bin) 83.5 m (bottom bin)	9.9 cm s^{-1} 12.2 cm s^{-1}	10.9 cm s^{-1}
CA6	13 m (top bin) 85 m (bottom bin)	20.5 cm s^{-1} 13.5 cm s^{-1}	15.8 cm s^{-1}

favorable wind stress in the time series data. In Figure 11 two examples of large upwelling and downwelling events have been highlighted by grey bands; one in ice-free conditions near the beginning of October 2002 and the other associated with the opening and closing of the flaw lead around the beginning of March 2003 (this is the event shown in Figure 4 and described in Williams *et al.,* 2008). For both events, with the onset of upwelling-favorable winds the velocity field responds quickly, and the salinity at 50 m deep at CA6 increases by 0.5 to 1 psu. The reversal in wind stress results in flow reversal and abrupt freshening.

7. Discussion

Upwelling-favorable wind forcing over the Canadian Beaufort Shelf will drive both focused upwelling at Cape Bathurst and uniformly-distributed upwelling across the outer shelf-break of the Canadian Beaufort Shelf. Both types of upwelling draw water from the nutrient-rich Pacific layer (cf. Carmack and Macdonald, 2002) and so both provide a source of new nitrate and silicate to the Canadian Beaufort Shelf. To begin to estimate their relative importance we can calculate the volume flux associated with each type. The maximum possible upwelling volume flux at Cape Bathurst is equal to the volume flux of the up-shelf flow over the Canadian Beaufort Shelf and is estimated as $\tau A/\rho r$ m^3 s^{-1}, whereas the upwelling volume flux across the outer shelf-break is just the Ekman transport times the length of the shelfbreak L_S and is estimated as $L_S\tau/\rho f$ m^3 s^{-1}. Equating these two volume fluxes leads to $L_S = Af/r$ where L_S is now the length of shelf for which the upwelling flux at Cape Bathurst is equal to the upwelling flux across the shelf-break (note that L_S is independent of the magnitude wind stress). For the Canadian Beaufort Shelf, the shelf is ~300 km long and $L_S \sim$ 500 km; hence the fluxes associated with upwelling at Cape Bathurst are comparable to shelf-break upwelling and are possibly equally important to new production on the shelf. In support of this we suggest that the higher nitrate concentrations found on the eastern half of the shelf in 1975 by Macdonald *et al.* (1987) were due to upwelling at the cape.

It is also necessary to consider how much upwelled nitrate actually reaches the euphotic zone and remains there long enough to be utilized by growing phytoplankton. Flux to the euphotic zone can be achieved either by upwelling directly to the surface or by upwelling onto the shelf and subsequent vertical mixing. The upwelling at Cape Bathurst can be directly to the surface and so likely increases primary productivity there. Evidence that efficient uptake occurs is reflected in the benthic community along the shelf break from Whale Bluff past Cape Bathurst to the mouth of Amundsen Gulf. This region shows very high numbers and diversity of benthic invertebrates (J. Grebmeier, pers. comm.; K. Conlan, pers. comm.) and has relatively high secondary benthic production estimates (P. Archambault, pers. comm.). The upwelled water may also be advected off the shelf by along-shelf flows. In particular, during downwelling-favorable wind-forcing the along-shelf flow should reverse and there is potential for upwelled water on the Canadian Beaufort Shelf to be advected off the shelf past Cape Bathurst, thus reducing the effect of

the upwelling. However, the presence of a rich benthic population at Cape Bathurst would suggest that water that upwells onto the shelf remains long enough to be utilized by phytoplankton and thus provide a source of carbon to the benthos.

While the divergent topography amplifies the upwelling at Cape Bathurst, its forcing ultimately depends on the wind. In general, persistent high pressure over the southern Beaufort Sea creates anticyclonic circulation and easterly/northeasterly wind stress over the Canadian Beaufort Shelf and so upwelling conditions are likely. NCEP reanalysis data show that annual mean wind stress over Canadian Beaufort Shelf has large interannual variation but is, on average, upwelling-favorable for about two out of every three years. The easterly/northeasterly winds are relatively persistent in April, May and June, but become more variable in July and August when cyclonic conditions may occur (Giovando and Herlinveaux, 1981). In September wind speeds increase and October has strong easterly winds. The severest storms tend to occur between September and November and often blow from the northwest (O'Brien *et al.,* 2006) giving downwelling-favorable wind stress over the Canadian Beaufort Shelf. November, December, January, February and March have variable wind stress but ice motion is generally towards the west during this time so that downwelling-favorable wind stress is often blocked (Williams *et al.,* 2006).

The question arises as to whether there are other locations wherein topographically enhanced wind-driven upwelling occurs. The topography of Cape Bathurst and Amundsen Gulf was created by a glacier cutting across the continental shelf and flowing into the Beaufort Sea during the last ice age; it is geomorphologically similar to a fjord. Mackenzie Trough is another example and there are numerous others across the Canadian Arctic Archipelago and other glaciated coastlines. Some of these locations may contain the necessary combination of isobath divergence and wind stress to create sites of recurrent upwelling.

8. Conclusions

Observations show enhanced upwelling at Cape Bathurst of nutrient-rich Pacific-origin water from about 110 m deep in Amundsen Gulf to the surface. Linear barotropic theory developed by Pringle (2002) suggests that the upwelling is a feature of the isobath divergence at Cape Bathurst. However, the extreme isobath divergence at Cape Bathurst suggests that both non-linear and stratified dynamics are important during upwelling. One drifter has rounded Cape Bathurst at 3 m s^{-1} during downwelling-favorable winds and this flow speed is expected to be attained during upwelling events also.

Acknowledgments. Thanks to Humfrey Melling and Fiona McLaughlin for their comments. Also thanks to Tom Weingartner and Mike Schmidt for the SeaWifs sea-surface temperature satellite images. The data for these images were obtained from the Ocean Color Data Processing Archive, NASA/Goddard Space Flight Center, Greenbelt, Maryland, USA. Funding for this work was provided by the Natural Sciences and Engineering Research Council of Canada and the Fisheries and Oceans Canada.

REFERENCES

Carmack, E. C. and E. A. Kulikov. 1998. Wind-forced upwelling and internal Kelvin wave generation in Mackenzie Canyon, Beaufort Sea. J. Geophys. Res., *103*(C9), 18447–18458.

Carmack, E. C. and R. W. Macdonald. 2002. Oceanography of the Canadian shelf of the Beaufort Sea: A setting for marine life. Arctic, *55*(Supp. 1), 29–45.

Chapman, D. C. and S. J. Lentz. 2005. Acceleration of a stratified current over a sloping bottom, driven by an along-shelf pressure gradient. J. Phys. Oceanogr., *35,* 1305–1307.

Chen, X. and S. E. Allen. 1996. The influence of canyons on shelf currents: a theoretical study. J. Geophys. Res., *101*(C8), 18043–18059.

Fairall, C. W., E. F. Bradley, D. P. Rogers, J. B. Edson and G. S. Young. 1996. Bulk parameterization of air-sea fluxes for tropical ocean—global atmosphere coupled—ocean atmosphere response experiment. J. Geophys Res, *101,* 3747–3764.

Fong, D. A. and W. R. Geyer. 2001. The response of a river plume during an upwelling favourable wind event. J. Geophys. Res., *106*(C1), 1067–1084.

Garrett, C., P. MacCready and P. Rhines. 1993. Boundary mixing and arrested Ekman layers: Rotating stratified flow near a sloping boundary. Ann. Rev. Fluid Mech., *25,* 291–323.

Giovando, L. F. and R. H. Herlinveaux. 1981. A discussion of factors influencing dispersion of pollutants in the Beaufort Sea. Pacific Marine Science Report 81-4, 198 pp.

Hyun, K. H. 2004. The effect of submarine canyon width and stratification on coastal circulation and across-shelf exchange. Ph.D. thesis, Old Dominion University, 108 pp.

Janowitz, G. S. and L. J. Pietrafesa. 1982. The effects of alongshore variation in bottom topography on a boundary current—(topographically induced upwelling). Cont. Shelf Res., *1,* 123–141.

Macdonald, R. W., C. S. Wong and P. E. Erickson. 1987. The distribution of nutrients in the southeastern Beaufort Sea: Implications for water circulation and primary production. J. Geophys. Res., *92*(C3), 2939–2952.

O'Brien, M. C., R. W. Macdonald, H. Melling and K. Iseki. 2006. Particle fluxes and geochemistry on the Canadian Beaufort Shelf: Implications for sediment transport and deposition. Cont. Shelf Res., *26,* 41–81.

Oke, P. R. and J. H. Middleton. 2000. Topographically induced upwelling off Eastern Australia. J. Phys. Oceanogr., *30,* 512–531.

Pease, C. H. 1987. The size of wind-driven coastal polynyas. J. Geophys. Res., *92,* 7049–7059.

Pringle, J. M. 2002. Enhancement of wind-driven upwelling and downwelling by alongshore bathymetric variability. J. Phys. Oceanogr., *32,* 3101–3112.

Swift, J. H. and K. Aagaard. 1976. Upwelling near Samalga Pass. Limnol. Oceanogr., *21,* 399–408.

Williams, W. J., E. C. Carmack and R. G. Ingram. 2007. The Physical Oceanography of Polynyas, Polynyas: Windows to the World. W. Smith and D. Barber eds., Elsevier Oceanography Series, *74,* 55–85.

Williams, W. J., E. C. Carmack, K. Shimada, H. Melling, K. Aagaard, R. W. Macdonald and R. G. Ingram. 2006. Joint effects of wind and ice motion in forcing upwelling in Mackenzie Trough, Beaufort Sea. Cont. Shelf Res., *26,* 2352–2366.

Williams, W. J., H. Melling, E. C. Carmack and R. G. Ingram. 2008. Kugmallit Valley as a conduit for cross-shelf exchange on the Mackenzie Shelf in the Beaufort Sea. J. Geophys. Res., *113,* C02007, doi:10.1029/2006JC003591.

Yankovsky, A. E. and D. C. Chapman. 1997. A simple theory for the fate of buoyant coastal discharges. J. Phys. Oceanogr., *27,* 1386–1401.

Received: *28 March, 2008;* revised: *31 October, 2008.*